Integrated Battery Lifetime and Energy Efficiency Driving Strategy for Electric Vehicles in Urban Environments

Bingbing Li, Weichao Zhuang, *Member*, *IEEE*, Sunan Zhang, Mingyang Chen, Guodong Yin, *Senior Member*, *IEEE*, Boli Chen, *Member*, *IEEE*

***Abstract*—Continuous traffic signal intersections in urban roads significantly increase vehicle energy consumption and the frequent acceleration and deceleration spur the degradation of electric vehicles (EVs) batteries. This paper proposes an integrated battery lifetime and energy efficiency driving strategy (IBE) based on a hierarchical framework for EVs in urban roads with multi-signalized intersections. In the upper layer, vehicles take into account global information from multiple traffic signals ahead in their travel direction to determine feasible phases time at each intersection. In the lower layer, a spatial-domain-based model predictive control (S-MPC) framework is introduced to achieve optimal control of the vehicle. Simulation results indicate that the proposed IBE strategy avoids stopping at red lights and, compared to two typical constant-speed strategies, can achieve a maximum improvement of 26.6% in battery lifetime and 10.5% in energy savings.**

***Index Terms*—Eco-driving, Model predictive control (MPC), Electric vehicles (EVs), Energy efficiency, Battery lifetime.**

I. Introduction

Against the backdrop of a continually expanding vehicle population and the escalating strain on energy resources within the road traffic system, there exists an imminent need to seek innovative solutions for addressing the issue of vehicle energy consumption [1]. Among the array of available options, eco-driving has prominently emerged as a pivotal approach to combat this challenge [2]. Eco-driving not only facilitates the reduction of fuel and battery consumption in vehicles but also holds the potential to curtail emissions, enhance traffic efficiency, and provide a viable pathway toward realizing sustainable transportation systems [3-5].

In recent years, especially in urban environments, advancements in vehicle-to-vehicle (V2V) and vehicle-to-infrastructure (V2I) communication technologies have significantly accelerated the dissemination of road environment information to vehicles [6]. This development has further propelled research into eco-driving strategies. Currently, extensive research endeavors have been undertaken to explore and assess diverse facets of eco-driving strategies for vehicles driven on urban roads [7-9]. Li et al. [10] pursued the objective of minimizing energy consumption in an internal combustion engine vehicle (ICEVs) by formulating a nonlinear mixed-integer optimal control problem (OCP). They successfully achieved energy-efficient vehicle operation through the application of the Legendre pseudospectral method in conjunction with the knotting technique. Jayawardana et al. [11] proposed an eco-driving strategy for signalized intersections based on reinforcement learning methods, and its generalizability was validated in mixed traffic scenarios. Chen et al. [12] developed a "1+n" hybrid vehicle platoon control strategy, which involves controlling a leading connected and automated vehicle to enhance the overall energy efficiency of the manually driven following vehicles, further improving road traffic efficiency. However, these studies have only focused on isolated signalized intersection scenarios. This type of eco-driving strategy, which only considers upcoming traffic signals, overlooks potential interference from other signal timings in the future. As a result, it can only achieve suboptimal control performance in terms of vehicle energy efficiency, especially in scenarios involving multiple traffic signals during long-distance driving. To this end, some scholars have also conducted research on eco-driving strategies in mult-intersection scenarios [13-15]. Chalaki et al. [16] presented a two-layer control framework designed for signal-free multi-intersections. In the upper layer, they planned the optimal arrival times for vehicles to maximize traffic flow efficiency, while in the lower layer, an OCP was formulated to determine the vehicle control actions. Arnau et al. [17] devised a driving strategy based on dynamic programming with a simplified model, which can determine the optimal speed profiles for a given horizon by knowing the information about the preceding traffic. Yang et al. [18] developed a modular and scalable driving system for multi-signal intersections that can be implemented in large-scale networks without significantly increasing computational complexity. Additionally, their research includes sensitivity analyses of variables such as demand levels and system market penetration, assessing their impact on system performance.

This work is supported by National Natural Science Foundation (NNSF) of China under Grants 52172383. (*Corresponding author: Weichao Zhuang*)

B. Li, W. Zhuang, S. Zhang, G. Yin are with School of Mechanical Engineering, Southeast University, Nanjing, 211189, China. (e-mail:bingbli@seu.edu.cn; wezhuang@seu.edu.cn; sunzhang@seu.edu.cn; ygd@seu.edu.cn.).

M. Chen, B. Chen is with the Department of Electronic and Electrical Engineering, University College London, WC1E 6BT London, U.K. (e-mail: uceemc4@ucl.ac.uk. boli.chen@ucl.ac.uk)

However, all of the aforementioned studies assume that the roads are flat considering only the effect of the traffic light, ignoring the impact of road gradients on vehicle energy efficiency. They generally assume that road gradients in urban areas are minimal, which is unpractical. For instance, in regions like Chongqing, China, and Scotland in the UK, urban roads exhibit significant gradients that have a profound impact on vehicle energy consumption. Furthermore, research focused on electric vehicles (EVs) as its subject has failed to consider the impact on battery lifespan. Batteries, being the most crucial components of EVs, pursuing energy efficiency in driving at the expense of battery longevity is inappropriate. Therefore, it is essential, in urban environments, to take road gradients and multiple traffic signals information into account and engage in comprehensive research on driving strategies for EVs aimed at improving both vehicle energy efficiency and battery lifetime.

This paper addresses the eco-driving control problem across multiple signalized intersections. A novel integrated battery lifetime and energy efficiency (IBE) control strategy is designed for a connected electric vehicles (CEV) to find the optimal driving profile, where vehicle energy efficiency and battery lifetime are co-optimized. The IBE strategy is framed in two layers: a feasible phase planning layer and a real-time vehicle control layer. The feasible phase planning layer uses global infromation from traffic signals and navigation system (distance, slopes, etc.) to determine viable time windows for each intersection with the aim of minimizing travel time. This breaks down the intricate path-level challenge into more manageable sub-tasks. On the other hand, the vehicle control layer employs a spatial-domain model predictive control (S-MPC) scheme. By solving the problem in the spatial domain, we can simultaneously optimize travel time, eliminating the need for an extra step typically required in the temporal domain. The spatial-domain approach also makes it straightforward to consider slopes, which can notably affect driving patterns but are often overlooked in existing studies [11-18]. Through this two-layer approach, we bypass the complex task of handling a mixed-integer nonlinear programming problem (MINLP), which often arises from signal phase and timing constraints [19]. As a result, the computational load is considerably alleviated.

The remainder of this paper is organized as follows. The energy-efficient driving problem in urban environments with multi-signalized intersections is formulated in Section II. Section III presents the framework of the proposed IBE driving strategy. Section IV shows the simulation results and evaluates the performance of IBE. The paper is concluded in Section V.

II. Problem Formulation

This section introduces the modelling framework, including the vehicle model, battery model, and traffic light model, and formulates the energy-efficent problem of the CEV at multiple signalized intersections.

A. Vehicle Model

The subject CEV, equipped with two hub motors, is neglected for lateral dynamics. Therefore, the longitudinal dynamics of the CEV in the spatial domain can be described as follows

$$\begin{cases} \dfrac{dv}{ds} = \dfrac{dv}{dt}\cdot\dfrac{dt}{ds} = \dfrac{a(s)}{v(s)} \\ \dfrac{dt}{ds} = \dfrac{1}{v(s)} \end{cases} \tag{1}$$

with

$$a(s) = \frac{1}{m}\left(\frac{2T}{r} - F_r(s) - F_v(s)\right) \tag{2}$$

$$F_r(s) = mgfcos(\theta(s)) + mgsin(\theta(s)) \tag{3}$$

$$F_v(s) = 0.5C_d\rho A v^2(s) \tag{4}$$

where m is the vehicle mass, s is the vehicle position, a and v are the acceleration and velocity of the vehicle, respectively. F_r is the road resistance, $F_v(s)$ is the air drag, r is the tire radius, T is the motor torque, g is the gravity constant, f, θ, and C_d are the rolling resistance factor, gradient and aerodynamic drag factor, respectively. A is the frontal area, ρ is the air density.

The energy consumption of the entire propulsion system can be expressed as

$$P_m = 2T\omega\eta_m^{-sgn(T)} \tag{5}$$

where ω is the motor speed, η_m is the motor working efficiency, as depicted in Fig. 1, which is accessible by a lookup table.

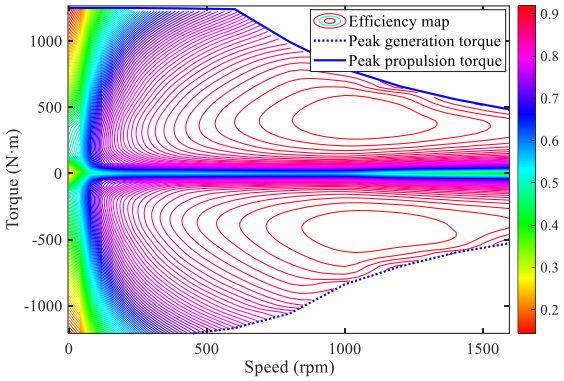

Fig. 1. Efficiency map the hub motor.

B. Battery Model

The electrical energy for CEV is provided by a LiFePO4 battery pack, and in this paper, an equivalent circuit model [20] represents it as follows

$$P_b = P_m + P_{aux} = U_{oc}I_b - I_b^2R_b \tag{6}$$

where P_{aux} is the auxiliary power. U_{oc} is the open-circuit voltage of the battery, I_b is the battery current, R_b is the internal resistance of the battery related to its state of charge (SOC). Likewise, in reference to the SOC dynamics the time domain [21], which can be written in the spatial domain as

$$\frac{d}{ds}\mathrm{SOC} = -\frac{I_b}{Q_b} = -\frac{U_{oc} - \sqrt{U_{oc}^2 - 4R_bP_b}}{2Q_bR_bv(s)} \tag{7}$$

where Q_b is the nominal capacity of the battery.

The maximization of battery life is one of the optimization objectives of this study. Therefore, a battery state of health (SOH) model is used to describe the battery lifetime degradation [22], which is presented as

$$\frac{d}{ds}\mathrm{SOH} = -\frac{|I_b|}{2Q_bN_c} = -\frac{\left|U_{oc} - \sqrt{U_{oc}^2 - 4R_bP_b}\right|}{4Q_bR_bN_cv(s)} \tag{8}$$

where N_c is the number of battery charge/discharge cycles.

C. Traffic Light Model

Vehicles traveling long distances in the urban environment are inevitably affected by traffic lights. For the sake of problem simplification, we assume that the timing of traffic lights is fixed. For a given signal light i, its signal cycle can be given as

$$T_c^i = T_r^i + T_g^i \tag{9}$$

where T_r^i and T_g^i are the ith red phase and green phase duration, respectively. It should be noted that yellow phase are counted as red light phase for safety reasons.

Fig. 2 illustrates two possible scenarios for the phase of signal light i. Here, we define the end time of the green phase as the starting moment of a single signal cycle. Assuming an initial time $t_0 = 0$, the cumulative number of cycles of signal i at time t can be calculated as

$$C^i = mod\left(\left(t - T_0^i\right), T_c^i\right) + 1 \tag{10}$$

with

$$T_0^i = \begin{cases} T_l^i + T_g^i & if\ H^i = 0 \\ T_l^i & if\ H^i = 1 \end{cases} \tag{11}$$

where $mod(\cdot)$ is the modulo operator. T_0^i the initial signal cycle length related to its initial phase H^i, $H^i = 0$ indicates that the initial phase is red, $H^i = 1$ means that the initial phase is green. T_l^i is the initial phase length.

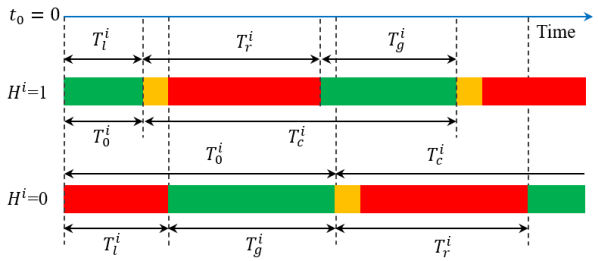

Fig. 2. The cycle clock time of the traffic light i.

Thus, the initial time of the phase of the ith signal light in a given cycle can be obtained as follows

$$t_r^{C^i} = \begin{cases} \begin{cases} \inf & C^i = 1, H^i = 1 \\ T_l^i + T_r^i(C^i - 2) + T_g^i(C^i - 2) & C^i > 1, H^i = 1 \end{cases} \\ \begin{cases} 0 & C^i = 1, H^i = 0 \\ T_l^i + T_r^i(C^i - 2) + T_g^i(C^i - 1) & C^i > 1, H^i = 0 \end{cases} \end{cases} \tag{12}$$

$$t_g^{C^i} = \begin{cases} \begin{cases} 0 & C^i = 1, H^i = 1 \\ T_l^i + T_r^i(C^i - 1) + T_g^i(C^i - 2) & C^i > 1, H^i = 1 \end{cases} \\ \begin{cases} 0 & C^i = 1, H^i = 0 \\ T_l^i + T_r^i(C^i - 1) + T_g^i(C^i - 1) & C^i > 1, H^i = 0 \end{cases} \end{cases} \tag{13}$$

D. Optimal Control Problem

The scenario investigated in this paper involves a CEV traveling on a long urban road with multiple multi-signalized intersections and road slops, as depicted in Fig. 3. The objective of this study is to develop a real-time EVs driving strategy aimed at improving vehicle energy efficiency and extending battery lifetime. Therefore, the control problem can be formulated as an (OCP) in the spatial domain

$$\min \int_{s_0}^{s_f} \left(\alpha_1 \frac{d}{ds}\mathrm{SOC} + \alpha_2 \frac{d}{ds}\mathrm{SOH}\right) ds \tag{14}$$

subject to (1) - (8), and

$$v(0) = v_0, t(0) = s_0 \tag{15}$$

$$\begin{cases} v(s) = 0 \text{ if } s = p^i \text{ and } t(p^i) \in \left[t_r^{C^i},\ t_r^{C^i} + T_r^i\right] \\ v(s) \neq 0 \text{ if } s = p^i \text{ and } t(p^i) \in \left[t_g^{C^i},\ t_g^{C^i} + T_g^i\right] \end{cases} \tag{16}$$

$$v_{min}(s) \le v(s) \le v_{max}(s) \tag{17}$$

$$T_{min}(s) \le T(s) \le T_{max}(s) \tag{18}$$

$$a_{min}(s) \le a(s) \le a_{max}(s) \tag{19}$$

where s_0 and s_f are the the start and end points, respectively. α_1 and α_2 are weighting factors. p^i is the ith signal light position. The subscripts max and min denote the maximum and minimum values of the corresponding variables, respectively. Eq. (15) is the initial state value of the system, Eq. (16) shows the effect of signal phase timing on vehicle motion state. Eq. (17) is the speed limit of the road. Eq. (18) is the physical constraint on the motor torque, and Eq. (19) is the acceleration constraint for driving comfort

It should be noted that the above OCP represents a typical MINLP due to the interference (16) caused by traffic signals [19]. Such a MINLP problem poses a significant challenge in computation, particularly in the receding horizon setting. To address this challenge, we propose a hierarchical framework that strikes a balance between optimality and computational efficiency.

III. IBE Driving Strategy Design

This section presents the overall framework of the proposed IBE driving strategy.

A. Feasible Phase Planning

In Fig. 3, the starting point of CEV is assumed to be $s_0 = 0$. In addition, the location of the road signal can be easily obtained based on the V2I technique, which is noted as $[p^1, p^2, \cdots, p^{N_l}]$. The distance between two consecutive signal light can be expressed as

$$L^i = \begin{cases} p^1 & i = 1 \\ p^i - p^{i-1} & i > 1 \end{cases} \tag{20}$$

The feasible phase planning at the upper level aims to make CEV to safely pass through the intersection without stopping in the green phase. Firstly, based on the established traffic light model, the green phase time range for the signal light i can be presented as

$$G^i = \sum_{c=1}^{n} \left[t_g^{C^i},\ t_g^{C^i} + T_g^i\right] \tag{21}$$

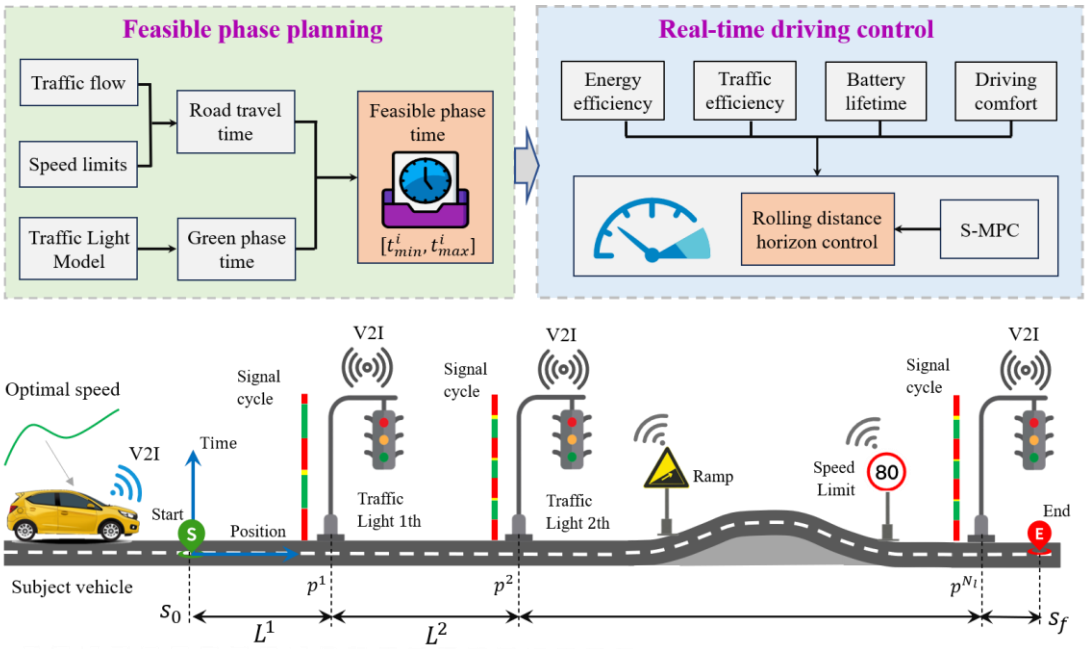

Fig.3. The problem description and proposed IBE driving strategy framework.

For the consideration of driving safety and traffic efficiency, the speed range of CEV is supposed to satisfy (17). The maximum speed is the road speed limit, and the minimum speed is set as a constant value based on the current average traffic speed of the given road. The average vehicle speed can be determined by prediction from historical traffic data or real-time accessed by platforms such as Google Maps. Thus, the CEV can traverse the intersection in a range of time that is

$$\Lambda^i = \sum_{k=1}^{N_i} \left[t^{k^i}_{gmin,}\, t^{k^i}_{gmax} \right] = G^i \cap D^i \tag{22}$$

with

$$D^i = \left[\frac{L^i}{v_{max}}, \frac{L^i}{v_{min}} \right] \tag{23}$$

where N_i is the number of feasible green phases for the ith signal light. $t^{k^i}_{gmin}$ and $t^{k^i}_{gmax}$ are the minimum and maximum time when the CEV passes the ith traffic light in the kth feasible green phases. D^i is the time interval to reach the intersection.

Currently, it is only the feasible travel time for the first intersection before CEV that has been planned. Next, we will consider feasible phase planning for multiple intersections. Based on the passing time of the ith signal, the time interval for the CEV to reach the (i+1)th signal can be calculated as follows

$$D^{i+1} = \sum_{k=1}^{N_i} \left[t^{k^i}_{gmin} + \frac{L^{i+1}}{v_{max}},\, t^{k^i}_{gmax} + \frac{L^{i+1}}{v_{min}} \right] \tag{24}$$

Hence, the feasible time slots of the $(i+1)$th signal light can be given as

$$\Lambda^{i+1} = \sum_{k=1}^{N_{i+1}} \left[t^{k^{i+1}}_{gmin,}\, t^{k^{i+1}}_{gmax} \right] = G^{i+1} \cap D^{i+1} \tag{25}$$

where N_{i+1} is the number of feasible green phases for the (i+1)th signal light.

In the same way, the feasible time for all traffic lights on the journey can be summarized as

$$\Lambda = [\Lambda^1, \Lambda^2, \cdots, \Lambda^n] \tag{26}$$

To minimize travel time and improve overall traffic efficiency, we choose the first feasible time slot as the target time interval for the vehicle to cross the traffic light, leading to

$$\widetilde{\Lambda} = \{[t^1_{min}, t^1_{max}], [t^2_{min}, t^2_{max}], \cdots, [t^n_{min}, t^n_{max}]\} \tag{27}$$

As a consequence, the whole OCP problem is decoupled into a sub-problem of single-signal intersection optimization.

B. Real-time Driving Control

This subsection describes the MPC control strategy based on the spatial domain. For each signal light, the terminal time range has been determined at the upper level as $[t^i_{min}, t^i_{max}]$, and this means that the feasible speed range is $[v^i_{f,min}, v^i_{f,max}] = \left[\frac{L^i}{t^i_{max}}, \frac{L^i}{t^i_{min}}\right]$. To ensure traffic efficiency, we assum the desired velocity is the maximum feasible speed, i.e., $v^i_d = v^i_{f,max}$. In each subproblem, the cost function for each rolling distance horizon in the S-MPC is formulated as follows

$$\begin{aligned} \alpha_1 J^i_1 + \alpha_2 J^i_2 + \alpha_3 J^i_3 = {} & \alpha_1 \big(\mathrm{SOC}(j|\varepsilon) - \mathrm{SOC}(j+N|\varepsilon)\big) \\ & + \alpha_2 \big(\mathrm{SOH}(j|\varepsilon) - \mathrm{SOH}(j+N|\varepsilon)\big) \\ & + \alpha_3 \big(v(j+N|\varepsilon) - v^i_d\big)^2 \\ & for\ all\ j = 1,2,\cdots N \end{aligned} \tag{28}$$

where j is the discrete index, N is the prediction horizon. $(j|\varepsilon)$ is the j-step-ahead prediction value at position ε. In particular, there is no time constraint after the CEV drives away from the last signal light. To ensure traffic efficiency, we set the ideal speed between this last traffic light and the end of the journey to the average speed of the road.

Thus, the OCP is described in each MPC update as follows

$$\min_{u} \alpha_1 J_1^i + \alpha_2 J_2^i + \alpha_3 J_3^i \quad (29)$$

subject to (18)-(19) and

$$v(j+1|\varepsilon) = v(j|\varepsilon) + \frac{a(j|\varepsilon)\Delta s}{v(j|\varepsilon)} \quad (30)$$

$$t(j+1|\varepsilon) = t(j|\varepsilon) + \frac{\Delta s}{v(j|\varepsilon)} \quad (31)$$

$$a(j|\varepsilon) = \frac{2T(j|\varepsilon)}{mr} - \frac{C_d \rho A v^2(j|\varepsilon)}{2m} - gsin\big(\theta(j|\varepsilon)\big) - gfcos\big(\theta(j|\varepsilon)\big) \quad (32)$$

$$v_{f,min}^i(j|s) \le v(j|s) \le v_{f,max}^i(j|s) \quad (33)$$

where the state variable $x = [v, t]$, and the control input is $u = T$. Δs is the sample distance. Eq. (30) and (31) are state equations. It should be seen that the vehicle is assumed to travel at a constant speed within each substage, which is due to the fact that s is small enough that the variations in speed are not significant. Eq. (33) is the velocity constraints of the vehicle.

IV. Simulation and Discussion

To validate the performance of the proposed driving strategy, a series of simulations are performed. All simulations are conducted on a personal computer with Intel® Core™ i7-10875H CPU @ 2.3 GHz and 16 GB RAM.

A. Simulation Setup

In the simulation, an urban road in Newcastle upon Tyne, England, with varying slopes is chosen as a simulated environment, as shown in Fig. 4. The road extends for approximately 9 km, encompassing a total of 6 traffic signal installations, while adhering to a maximum speed limit of 80 km/h. It is noteworthy to mention that the data regarding road gradients and average traffic speeds are obtained through Google Maps. The experiments are conducted at approximately 14:00 local time, during which the real-time average vehicle speed on the road is 50 km/h. To realize the trade-off between traffic efficiency and energy savings, the minimum speed is assumed to be 20 km/h. In the S-MPC, the relevant parameters are set: Δs = 5 m, Q = 50 m, N = 10, a_{max} = 2 m/s^2, a_{min} = -2 m/s^2, and the vehicle initial velocity v_0 = 50 km/h. In addition, the main parameters of the CEV are listed in Table I, and the light signal positions and the signal phasing and timing are shown in Table II.

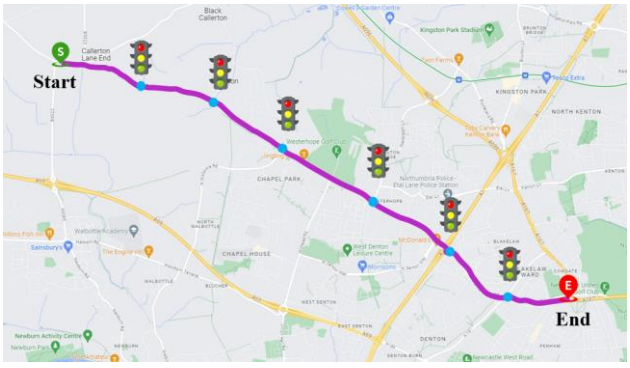

Fig. 4. The experimental route in Newcastle upon Tyne, England.

TABLE I
SUBJECTIVE VEHICLE PARAMETERS

Component	Parameter	Symbol	Value
Vehicle	Mass	m	2000 kg
	Accessory power	P_{aux}	400 W
	Tire radius	r	0.36 m
	Frontal area	A	2.5 m^2
	Air drag coefficient	C_d	0.28
	Rolling resistance coefficient	f	0.018
	Air density	ρ	1.206 kg/m^3
	Gravity factor	g	9.81 m/s^2
Motor	Maximum Torque	T_{max}	1225 Nm
	Minimum Torque	T_{min}	-1200 Nm
Battery	Nominal capacity	Q_b	125 Ah
	Internal resistance	R_b	0.32 Ω
	Lifetime cycle	N_c	2500
	Open-circuit voltage	U_{oc}	360 V

To quantify the performance of the proposed IBE driving strategy, a common CS strategy is used as a benchmark. Therefore, for a fair comparison, we improve the CS strategy by only allowing the vehicle to drive at a constant speed between two substages to ensure that the vehicle passes through the traffic lights. The speed variations between sub-stages are ignored. The speeds of the CS strategy are set to the maximum and minimum of the feasible speeds, and the two strategies are denoted as CS-U and CS-L, respectively.

TABLE II
ROAD AND SIGNAL LIGHT PARAMETERS

Number	Position	Red phase time	Green phase time
Start	0 m	--	--
1	1200 m	35	30
2	2200 m	65	40
3	3700 m	62	45
4	5100 m	55	37
5	6400 m	65	40
6	8000 m	67	55
End	9000 m	--	--

B. Results

Fig. 5 displays the vehicle speed trajectories for three driving strategies. It can be observed that the speed of IBE remains within the specified speed range and fluctuates continuously with changes in road slope. Specifically, in the 0-1000 m range of Fig. 5, we can see that the vehicle speed reaches a minimum when it arrives at the top of the slope. This manner greatly improves the vehicle energy efficiency by utilizing the gravitational potential energy to increase the kinetic energy.

Table III presents a performance comparison among three driving strategies. It is evident that IBE demonstrates a notable improvement in both battery lifetime and vehicle energy efficiency compared to the other two strategies. In comparison to CS-U, IBE achieves a remarkable 10.5% energy savings and a 26.6% energy saving. Relative to CS-L, while the energy efficiency of IBE increases by only 3.4%, the battery lifetime can still be extended by 21.2%, and driving time significantly reduced.

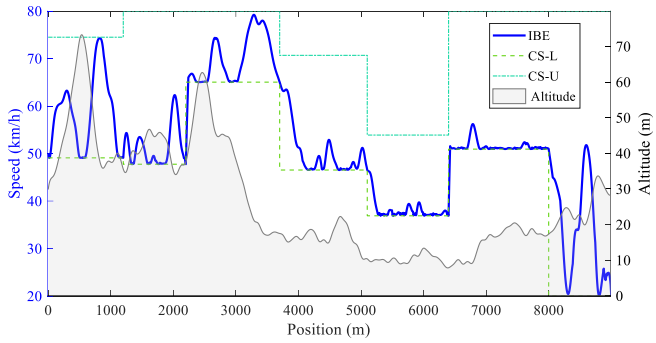

Fig. 5. Vehicle velocity trajectories for different driving strategies with corresponding road slope.

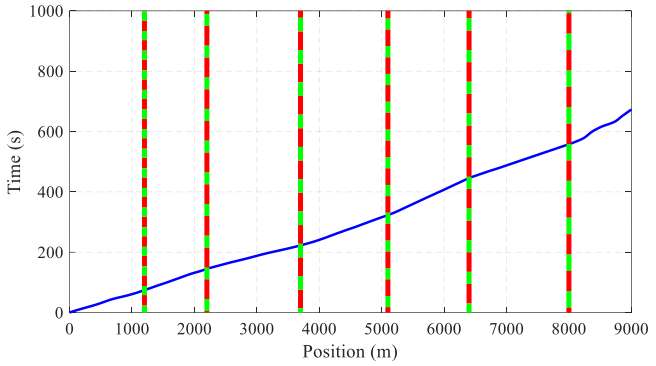

(a) Position trajectories.

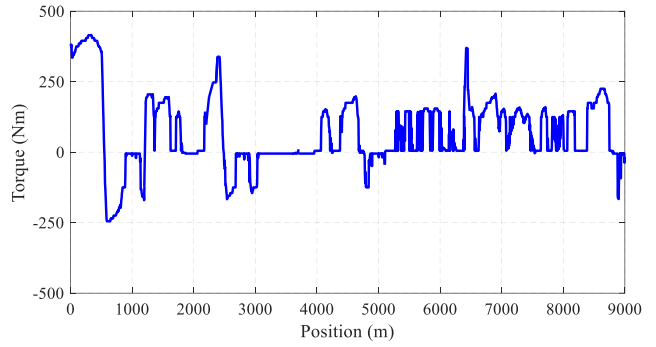

(b) Torque trajectories.

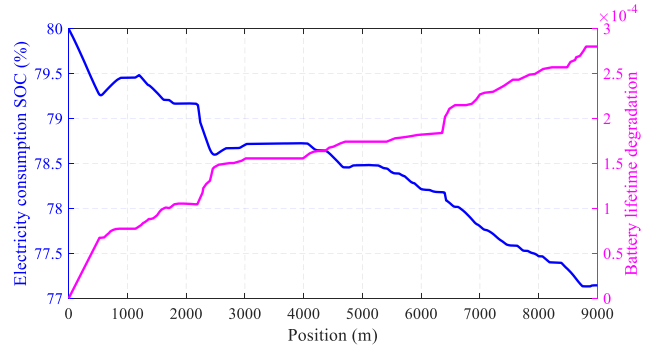

(c) SOC trajectories and SOH trajectories

Fig. 6. The performance of the IBE driving strategy.

Fig. 6 further illustrates the vehicle position, torque, SOC variations, and battery lifetime degradation trajectory under the IBE driving strategy. It can be observed that, despite traffic signal disruptions along the road, IBE ensures that the vehicle passes through traffic lights in the green phases, preventing energy dissipation due to vehicle stops. It is worth noting that the proposed strategy may occasionally require the vehicle to apply rapid acceleration, which appears to be energy inefficient (see, for example, at 6500 m). This is due to the design of the upper-level controller in the present paper, aiming to have the vehicle pass each traffic lights during the earliest possible green phase to improve traffic flow. A more balanced scheme that considers both traffic and vehicle efficiency is envisaged to be done in future work.

TABLE III
PERFORMANCE COMPARISON OF DIFFERENT DRIVING STRATEGIES

Performance	IBE (%)	CS-U (%)	CS-L (%)
SOC change	2.8	3.094 (↑ 10.5%)	2.895 (↑ 3.4%)
SOH change	0.0278	0.0352 (↑ 26.6%)	0.0337 (↑ 21.2%)

Note: The values inside the parentheses are the performance improvement of the IBE relative to other strategies.

V. CONCLUSION

This paper introduces a layered IBE driving strategy aimed at enhancing the battery lifetime and energy efficiency of EVs in urban environments. Compared to the two typical CS strategies, the IBE strategy achieves energy savings of 3.4% and 10.5% and battery lifespan improvements of 21.2% and 26.6%, respectively. In additon, the IBE strategy ensures non-stop passage of vehicles at traffic signal intersections, thereby improving traffic efficiency. In the future, we will conduct real-world experiments to validate the feasibility of the strategy.

REFERENCES

[1] J. Han, D. Shen, D. Karbowski, and A. Rousseau, "Leveraging multiple connected traffic light signals in an energy-efficient speed planner," *IEEE Contr. Syst. Lett*., vol. 5, no. 6, pp. 2078-2083, Dec. 2021.

[2] D. Shen, D. Karbowski, and A. Rousseau, "A minimum principle-based algorithm for energy-efficient eco-driving of electric vehicles in various traffic and road conditions," *IEEE Trans. Intell. Veh.*, vol. 5, no. 4, pp. 725-737, Dec. 2020.

[3] Y. Luo, K. Li, and S. Li, "Green light optimal speed advisory for hybrid electric vehicles," *Mech. Syst. Signal Pr.*, vol. 87, no. 6, pp. 30-44, Jun. 2016.

[4] S. Mousa, S. Ishak, R. Mousa, J. Codjoe, M. Elhenawy, "Deep reinforcement learning agent with varying actions strategy for solving the eco-approach and departure problem at signalized intersections," *Transp Res Rec.*, vol. 2674, no. 8, pp. 119-131, Jul. 2020.

[5] Q. Lin, S. Li, S. Xu, X. Du, D. Yang, K. Li, "Eco-driving operation of connected vehicle with V2I communication among multiple signalized intersections," *IEEE Intell Transp Syst Mag.*, vol. 13, no. 1, pp. 107-119, Sep. 2021.

[6] X. He, and X. Wu. "Eco-driving advisory strategies for a platoon of mixed gasoline and electric vehicles in a connected vehicle system," *Transport. Res. D-tr. E.*, vol. 63, no. 5, pp. 907-922, Aug. 2018.

[7] B. Liu, C. Sun, et al. "Bi-level convex optimization of eco-driving for connected fuel cell hybrid electric vehicles through signalized intersections," *Energy*, vol. 252, Apr. 2022, Art. no. 123956.

[8] X. Shan, C. Wan, and P. Hao, "Connected eco-driving for electric buses along signalized arterials with bus stops," *IET Intelligent Transport Systems*., Vol. 17, no. 3, pp. 579-591, Mar. 2023.

[9] X. Wei, J. Leng, C. Sun, W. Huo, Q. Ren, and F. Sun, "Co-optimization method of speed planning and energy management for fuel cell vehicles through signalized intersections," *J. Power Sources,* vol. 518, Jan. 2022, Art. no. 230598.

[10] S. E. Li, S. Xu, et al. "Eco-departure of connected vehicles with V2X communication at signalized intersection," *IEEE Trans. Intell. Veh.*, vol. 64, no. 12, pp. 5439-5449, Dec. 2015.

[11] V. Jayawardana and C. Wu, "Learning eco-driving strategies at signalized intersections," 2022 *European Control Conference (ECC), London, United Kingdom*, 2022, pp. 383-390, doi: 10.23919/ECC55457.2022.9838000.

[12] C. Chen, J. Wang, et al. "Mixed platoon control of automated and human-driven vehicles at a signalized intersection: Dynamical analysis and optimal control," *Transp Res Part C Emerg Technol.*, vol. 127, Jun. 2021, Art. no. 103138.

[13] X. Zeng, J. Wang. "Globally energy-optimal speed planning for road vehicles on a given route," *Transp. Res. Part C: Emerg. Technol.* vol. 93, pp. 148-160, May. 2018.

[14] M. Wegener, L. Koch, M. Eisenbarth, J. Andert. Automated eco-driving in urban scenarios using deep reinforcement learning. *Transp. Res. Part C: Emerg.Technol.* vol. 126, May. 2021, Art. no. 102967.

[15] C. Sun, J. Leng and F. Sun, "A Fast Optimal Speed Planning System in Arterial Roads for Intelligent and Connected Vehicles," *IEEE Internet Things J.*, vol. 9, no. 20, pp. 20295-20307, Oct. 2022.

[16] B. Chalaki and A. A. Malikopoulos, "Optimal Control of Connected and Automated Vehicles at Multiple Adjacent Intersections," *IEEE Trans Control Syst Technol*, vol. 30, no. 3, pp. 972-984, May 2022.

[17] F. J. Arnau, B. Pla, P. Bares and A. T. Perin, "Eco-Driving Optimization of a Signalized Route With Extended Traffic State Information," *IEEE Intell Transp Syst Mag.*, vol. 15, no. 4, pp. 35-45, Jul. 2023.

[18] H. Yang, F. Almutairi and H. Rakha, "Eco-Driving at Signalized Intersections: A Multiple Signal Optimization Approach," *IEEE Intell Transp Syst.*, vol. 22, no. 5, pp. 2943-2955, May 2021.

[19] M. Tajalli and A. Hajbabaie, "Traffic Signal Timing and Trajectory Optimization in a Mixed Autonomy Traffic Stream," *IEEE Intell Transp Syst.*, vol. 23, no. 7, pp. 6525-6538, July 2022.

[20] V. Johnson, " attery performance models in A VISOR," *J.Power Sources.*, vol. 110, no. 2, pp. 321-329, Jun. 2002.

[21] F. Ju, N. Murgovski, W. Zhuang, Q. Wang and L. Wang, "Predictive Cruise Controller for Electric Vehicle to Save Energy and Extend Battery Lifetime," *IEEE Trans. Intell. Veh.*, vol. 72, no. 1, pp. 469-482, Jan. 2023.

[22] J. Wang et al., "Cycle-life model for graphite-lifepo4 cells," *J. Power Sources*, vol. 196, no. 8, pp. 3942-3948, 2011.